

Structural and electronic properties of Si/Ge nanoparticles

Abu Md. Asaduzzaman* and Michael Springborg†

Physical and Theoretical Chemistry,

University of Saarland, D-66123 Saarbrücken, Germany

(Dated: October 12, 2018)

Abstract

Results of a theoretical study of the electronic properties of (Si)Ge and (Ge)Si core/shell nanoparticles, homogeneous SiGe clusters, and Ge|Si clusters with an interphase separating the Si and Ge atoms are presented. In general, (Si)Ge particles are more stable than (Ge)Si ones, and SiGe systems are more stable than Ge|Si ones. It is found that the frontier orbitals, that dictate the optical properties, are localized to the surface, meaning that saturating dangling bonds on the surface with ligands may influence the optical properties significantly. In the central parts we identify a weak tendency for the Si atoms to accept electrons, whereas Ge atoms donate electrons.

PACS numbers: 73.22.-f, 61.46.Df, 73.61.Le, 36.40.-c

* e-mail: a.asaduzzaman@mx.uni-saarland.de

† e-mail: m.springborg@mx.uni-saarland.de

I. INTRODUCTION

Traditionally, materials properties have been controlled by varying structure and composition of the materials. During the last quarter of a century a new parameter has been added, i.e., size. The fact that the materials properties change drastically when the dimension of the materials becomes comparable with the typical length scale of the phenomenon of interest together with the ability to control the production of materials in this size range has led to the development of ‘nano-science’.

One of the materials classes where materials in the nm range are expected to have a large impact on the development of new and/or better devices is semiconductors. For those, modified electronic properties may show up when the size of the nanocrystals is comparable with the spatial extension of the excitons. For instance, the light emission properties of semiconductor nanocrystal quantum dots, specifically the tuning of color afforded by the quantum size effect, is important for application of these materials in light emitting devices^{1,2,3,4} and as biological fluorescence markers.^{5,6,7}

A further development which has opened up new possibilities to control and vary the materials properties is the successful production of core/shell nanoparticles, consisting of a core of one material coated by a well-defined shell layer of another material. These systems exhibit unique and advanced properties over single-component nanoparticles, making them attractive for use in a wide range of real-world applications, and are therefore of extensive scientific and technological interest. In the last few years, much effort has been focused on the synthesis, fabrication, and characterization of the core/shell structured semiconductor heterostructures with tailored properties. The growth of the shell on the core material to form a core/shell heterostructures has been successfully demonstrated on the surface reconstruction of nanostructured material. Among the ingredients that dictate the electronic, electrical, optical, and chemical properties of core/shell nanostructures, the surface-to-volume ratio, the shell type and shell thickness are important, although a precise understanding of the relations between structure, size, and composition on the one hand and property on the other hand is lacking.

Recently, Lauhon *et al.*⁸ reported the epitaxial growth of crystalline silicon-germanium and germanium-silicon core/sheath structures. Despite a 4% lattice mismatch of the macroscopic crystalline systems, the experimental study demonstrated that for Si core nanowire,

the Ge shell is fully crystallized at low temperatures and for a Ge core nanowire, an amorphous Si shell is formed initially and after thermal annealing the shell becomes crystallized. In another study, Malachias *et al.*⁹ experimentally showed the formation of Ge domes with a Si core and a Ge shell. Kolobov *et al.*¹⁰ in their experimental study showed the formation of nanocrystals of a Ge core with a SiGe shell. On the other hand, there are few experimental and theoretical studies on core/shell materials reported.^{11,12,13} Most studies on core/shell studies have considered binary compounds like CdSe/ZnS, ZnS/CdS, CdSe/CdS, etc. Core-shell studies on pure elements are very scarce. Recently, Musin and Wang¹⁴ reported a theoretical study on the epitaxial Si-Ge core/shell structure, a theoretical realization of the experimental work of Lauhon *et al.*

In this paper, we present the results of a theoretical study of structural and electronic properties of naked Si-Ge and Ge-Si core/shell nanoparticles. Musin and Wang took into consideration the epitaxial growth of Si-Ge core/sheath nanowires and studied the compositional dependency of the structural parameters and the band gap energy. Here, we have considered naked Si-Ge and Ge-Si core/shell nanoparticles for which we assumed that the structure is related to that of a spherical cut-out of the infinite crystal with a zincblende- or diamond-like structure. Although our assumption may affect the results of the calculations, we believe that by considering a larger number of sizes (almost 100 sizes with up to in total almost 200 atoms) our study allows for drawing general conclusions on those systems. Starting with a small core of only 8 atoms and a thin shell of 24 atoms we have gradually increased the sizes of both core and shell. In order to find out how the properties of core/shell particles depend on the two elements, we have, in addition, carried out calculations on pure Si clusters, pure Ge clusters, homogeneous SiGe clusters, and spherical structures with half of the sphere made up of Si and the other half made up of Ge atoms (Si|Ge). A representative example of a core/shell particle as well as of homogeneous SiGe and of a Si|Ge particle is depicted in Fig. 1. We mention that the experimentally studied systems are considerably larger (containing up to several 1000s of atoms), which is very difficult to study theoretically. Therefore, in this study we have limited ourselves to a detailed study of different core/shell structures along with pure Si and Ge, homogeneous SiGe, and Si|Ge systems with up to around 200 atoms, which is around 2 nm in radii. We have optimized all the structures to their nearest local total-energy minima whereby all atoms were allowed to move.

II. COMPUTATIONAL OUTLINE

We have used a parameterized density-functional tight-binding method that has been described in detail elsewhere.^{15,16,17} The total energy relative to the isolated atoms of a given system is written by

$$E_b = \sum_i \epsilon_i - \sum_{jk} \epsilon_{jk} + \frac{1}{2} \sum_{k \neq l} U_{kl} (|\vec{R}_k - \vec{R}_l|) \quad (1)$$

Here, ϵ_i is the energy of the i th orbital for the system of interest and ϵ_{jk} is the energy of the j th orbital for the isolated k th atom. U_{kl} is a pair potential between the k th and l th atom. The valence single-particle eigenfunctions $\psi_i(\vec{r})$ to the Kohn-Sham equation are expanded in a set of atom-centered basis functions $\chi_{klm}(\vec{r})$, where k denotes the atom and (l, m) the angular dependence. The effective one-electron potential in the Kohn-Sham Hamiltonian is approximated as a superposition of the atomic potentials of the corresponding neutral atoms, and it is assumed that the matrix elements $\langle \chi_{k_1 l_1 m_1} | V_j | \chi_{k_2 l_2 m_2} \rangle$ (with V_j being the atomic potential at atom j) are vanishing unless $k_1 = j$ or $k_2 = j$. Thus, only two-center Hamiltonian matrix elements are considered and calculated exactly within the Kohn-Sham basis for the diatomic molecules. Finally, the pair potentials U_{kl} are determined so that the binding energy curve of the diatomics are well reproduced. Only the $3s$ and $3p$ functions of Si and the $4s$ and $4p$ functions of Ge were explicitly included in the calculations, whereas all other electrons were treated within a frozen-core approximation.

It is obvious that, the approach we are using has been designed for the smallest possible systems Si₂, Ge₂, and SiGe. We have verified the capability of this method to do calculations for larger systems by studying some characteristics of bulk Si and Ge. The experimental lattice constants of crystalline Si and Ge are 5.43 and 5.66 Å, respectively, whereas our calculations give 5.46 and 5.71 Å, respectively, i.e., within less than 1% of the experimental values. The experimental band gaps of bulk Si and Ge are 1.12 and 0.66 eV, respectively, and our calculated values are 1.097 and 0.65 eV, respectively which are also close to the experimental values. Here, the standard problem of density-functional calculations to yield too small band gaps seems to be absent, mainly due to the fact that our basis set is minimal in size.

In addition to the clusters containing both Si and Ge atoms, we have also studied small clusters of pure Si or Ge, separately. Among the different arrangements of three atomic Si

and Ge clusters, clusters with C_{2v} symmetry are those of the minimum energy configuration. Clusters with D_{2h} symmetry are the minimum energy structures among the four atomic clusters for both Si and Ge. Earlier theoretical studies on Si and Ge¹⁸ and on Si²⁰ also reported those minimum energy structures.

In all cases we relaxed initial structures that we constructed by cutting out a spherical part of a diamond-like crystal. The initial lattice constant was taken as that of the pure crystalline systems (for the pure Si and Ge clusters) or as the average of those two values (for the heteroatomic structures). The center of the sphere was taken as the midpoint of a nearest-neighbor bond, giving that the number of atoms would be 2, 8, 20, 32, 38, 56, 74, 86, 116, 130, 166, or 190 if 1, 2, ..., 12 atomic shells were included in the initial structure (here, we define an atomic shell as being the set of atoms that has the same distance to the center of the spherical cut-out in the initial structure). Subsequently, the initial structure was allowed to relax to its closest total-energy minimum, whereby all atoms (i.e., both in the inner part and in the surface region) were displaced until the forces on them vanish.

III. RESULTS

We studied in total 95 different structures. Each of those structures consists of $N_{\text{Si},i}$ Si atoms and $N_{\text{Ge},i}$ Ge atoms, $i = 1, 2, \dots, 95$. Using a least-squares fit we approximated the binding energy of those 95 structures by a sum of atomic energies,

$$E_{b,i} \simeq E_{\text{Si}}N_{\text{Si},i} + E_{\text{Ge}}N_{\text{Ge},i} \equiv \tilde{E}_{b,i}. \quad (2)$$

Subsequently, we defined one stability energy for each cluster,

$$\Delta E_1 = E_{b,i} - \tilde{E}_{b,i} \quad (3)$$

which is the more negative the more stable the cluster is. Finally, we analyse this quantity per atom, i.e.,

$$\Delta E_1/N = \Delta E_1/(N_{\text{Si},i} + N_{\text{Ge},i}). \quad (4)$$

We also considered the stability energy

$$\Delta E_2/N = E_{b,i}/(N_{\text{Si},i} + N_{\text{Ge},i}). \quad (5)$$

Each of those quantities is analysed as a function of the number atomic shells either in the core, in the shell, or in the complete nanostructure. I.e., with N_t being the total number

of atomic shells, $1 \leq N_t \leq 12$, for the core/shell particles we have N_c atomic shells in the core and $N_s = N_t - N_c$ shells in the shell part, whereas $N_s = N_t, N_c = 0$ for the homogeneous SiGe clusters and for the Si|Ge nanoparticles.

The fit of Eq. (2) resulted in $E_{\text{Si}} = -2.37$ eV and $E_{\text{Ge}} = -3.58$ eV. The fact that E_{Ge} is more negative than E_{Si} implies that it is energetically more favorable for Ge atoms than for Si atoms to be incorporated into those nanostructures, although the difference in the two energies is relatively small. On the other hand, the cohesive energy of the solids equals 4.63 and 3.85 eV/atom for Si and Ge, respectively (see, e.g., [19]), giving that for the elemental solids it is energetically more favorable for Si than for Ge atoms to be incorporated into the solids. The difference between our results and those for the elemental solids may be due to the differences in the systems (both with respect to composition and regarding size) and in the finite number of structures that we include in our fit.

The fact that $E_{\text{Ge}} < E_{\text{Si}}$ also means that when comparing ΔE_1 and ΔE_2 , the larger the number of Ge atoms is compared with that of Si atoms, the lower is ΔE_2 compared with ΔE_1 .

In Figs. 2 and 3 we show the two energies $\Delta E_1/N$ and $\Delta E_2/N$ as a function of the number of shells in either the core region, in the shell region, or in the complete cluster.

First, the results for the Si|Ge and the homogeneous SiGe nanosystems show clearly that the latter is more stable than the former. In addition, in both cases the binding energy per atom is a decaying function of the size of the system. This behavior is often found for clusters, and can be related to the presence of the surface atoms for which the appearance of dangling bonds and lower coordinations lead to energetically less favorable situations. When the system size is increased, the relative importance of the surface is reduced, leading to an overall decaying total energy per atom as a function of size. The fact that the precise number of surface atoms is not completely regular as a function of cluster size can explain the deviations from a completely smooth behavior.

Comparing Figs. 2(b) and 3(b) the finding that the latter is fairly unstructured, whereas the former shows a clear decaying behavior as function of size suggests that for the (Ge)Si systems, i.e., a Ge core covered with Si shells, the total energy for this system depends only marginally on its size.

On the other hand, Figs. 3(d) shows that for the (Ge)Si nanoparticles the variation in the total energy is mainly determined by the number of atomic Si shells in the shell part

and largely independent of the number of atomic Ge shells in the core region. A similar result is found for the (Si)Ge nanoparticles in Fig. 2(c) with, however, some few exceptions that are recovered in all results for these systems, i.e., in Figs. 2(a,c,e) and Figs. 3(a,c,e). It turns out that these exceptions are among the smallest systems we have studied with only two atomic shells of Si covered with a low number of Ge shells. We mention that the systems with no atomic Si shells of Si, are less stable, so that the (Si)Ge nanoparticles with two atomic shells of Si covered with a small number of Ge shells indeed are the most stable systems of the present study. We do not have a precise explanation for this finding.

A further result can be seen when comparing the (Si)Ge core/shell systems with the (Ge)Si ones: the former are more stable than the latter. Since the (Si)Ge systems contain a Ge surface, whereas the (Ge)Si systems contain a surface of Si atoms, this result may be a simple consequence of the lower surface energy of Ge compared with that of Si (see, e.g., [21]).

The HOMO-LUMO gap, E_{gap} , (i.e., the energy gap between the highest occupied molecular orbital and the lowest unoccupied molecular orbital) is shown in Fig. 4 similarly to Figs. 2 and 3. With no exception the gap is significantly smaller than those of the elemental solids and in many cases it is even close to vanishing. The systems with the largest gaps are the core/shell nanoparticles with the smallest number of atomic shells in the complete system as well as the Si|Ge systems. Marsen *et al.*,^{23,24} in their experimental study, showed that the band gap of small silicon clusters is larger (the largest value being 0.45 eV) than that of the large clusters (most clusters have gap ranging from 0.025 to 0.10 eV) and the gap is size dependent. Besides that, they observed essentially no correlation between size of the gap and size of the cluster, which is in good agreement with our results.

In an earlier work on a number of stoichiometric II-VI and III-V nanoparticles we found a close correlation between the HOMO-LUMO gap and the stability.²² In order to explore whether a similar correlation exists here, we show in Fig. 5 E_{gap} as a function of $\Delta E_1/N$. It is clear that no correlation is found in the present case. Replacing $\Delta E_1/N$ by $\Delta E_2/N$ does not change this conclusion.

Ge/Si nanowires with a Si sheath covering a Ge core have been of some interest recently (see, e.g., [25]), also as active components in semiconductor devices. In these, it is assumed that a hole gas is formed in the Ge wire. If the systems were isolated, this would imply a net electron transfer from Ge to Si, which, then, also may occur for the system of the present

study. In order to study this, we first determine the center of the cluster with n Si atoms and m Ge atoms,

$$\vec{R}_0 = \frac{1}{n+m} \sum_{j=1}^{n+m} \vec{R}_j, \quad (6)$$

and, subsequently, for each atom its so-called radial distance

$$r_j = |\vec{R}_j - \vec{R}_0|. \quad (7)$$

Subsequently, we plot the Mulliken gross populations of the individual atoms as a function of the radial distance; cf. Fig. 6. Indeed, it is seen that for the (Si)Ge core/shell particles there is a slight tendency for the atomic populations on the Si atoms to be larger than 4, whereas for the (Ge)Si core/shell particles, the Ge atomic populations are on the average below 4. On the other hand, in the shell region, the trend is less clear. However, in total, these core/shell systems do show tendency towards electron- or hole-gas formation in the central part, depending on whether Si or Ge is the material of the core. The finding that the atomic populations deviate most from the value of 4 for the atoms closest to the surface is also observed for the Si|Ge systems. For the homogeneous SiGe systems we also observe a small electron transfer from Ge to Si in the central part, which, however, not is the case for the central parts of the Ge|Si systems.

Much of the interest in semiconductor nanoparticles is connected with their partly controllable optical properties that first of all are dictated by the properties of excitons, which in turn are determined by the energy and the charge distribution of the orbitals closest to the Fermi level, i.e., the HOMO and the LUMO. Optical relaxation processes strongly depend on the spatial distribution of these orbitals. Therefore, we shall study these. To this end we construct for any orbital the density

$$\rho_i(\vec{r}) = \sum_j N_{ij} \left(\frac{2\alpha}{\pi} \right)^{3/2} \exp[-\alpha(\vec{r} - \vec{R}_j)^2]. \quad (8)$$

Here, N_{ij} is the Mulliken gross population for the j th atom and i th orbital, and α is chosen ‘reasonably’, so that illustrative figures result.

Fig. 7 shows the resulting schematic representation of this radial dependence of the HOMO and LUMO. It is seen that in most cases, both the HOMO and the LUMO are localized to the surface of the clusters, irrespectively of whether we consider (Si)Ge or (Ge)Si systems. In an earlier study on CdSe/CdS core/shell nanoparticles²⁶ it was found that one

may find systems for which the LUMO and the HOMO were localized in different parts (i.e., in the shell and in the core) of the system, but this is obviously not the case for the present systems. Since the gap of crystalline Ge is smaller than that of crystalline Si, and since the HOMO and LUMO of the present systems are located to the surface region, it may be suggested that the gap of the (Si)Ge particles is smaller than that of the (Ge)Si systems. Actually, such a difference has been found for the pure Ge and Si systems by Melnikov and Chelikowsky.²⁷ However, in the present study such a trend is only very marginally found for the core/shell systems, which is in agreement with the theoretical results of Musin and Wang¹⁴ who studied Ge/Si and Si/Ge core/sheath nanowires. Moreover, Musin and Wang found a larger band gap than those of the pure, crystalline elements for all systems, which most likely is due to the passivation of the surface included in their study. This once again indicates that without passivation the frontier orbitals are localized to the surface region.

Also for the homogeneous SiGe systems the frontier orbitals are located to the surface, as can be seen in Fig. 8. For the Si|Ge systems we find also this behavior, cf. Fig. 9. In both cases we find that the HOMO is localized to both Si and Ge atoms, whereas the LUMO is localized mainly to the Ge atoms.

IV. CONCLUSION

In this paper, we have presented the results of our study of the structural and electronic properties of naked (Si)Ge and (Ge)Si core/shell nanoparticles together with those of pure Si and Ge, homogeneous SiGe and Si|Ge systems with a diameter of up to around 2 nm. The interesting properties critically depend on the size of core and shell and also on the type of core and shell atoms. Although we did not enter a detailed discussion of this issue, we emphasize that our results on pure Si and Ge clusters, in particular concerning the reduced band gap compared with the crystalline material, are in excellent agreement with results of other experimental and theoretical studies.

Due to difference in surface energy, (Si)Ge core/shell systems are more stable than are (Ge)Si systems. Moreover, the stability of the (Si)Ge systems was quite well described in terms of the quantity ΔE_1 as a function of the number of core shells, whereas ΔE_2 as a function of the number of core shells gave a good description of the stability of the (Ge)Si systems.

We did observe a marginal tendency of a Ge→Si electron transfer, irrespectively of which system was forming the core and which the shell. A similar effect was not found for the homogeneous SiGe systems, but for the interface Si|Ge systems.

In all systems, the (unpassivated) surface was dictating the properties of the frontier orbitals. The latter were localized to the surface, and their energies occurred in the energy gap of the pure, infinite crystals, leading to quite low band gaps. Therefore, surface passivation could be a useful means of tuning the optical properties of these systems. In contrast to our earlier results on naked AB semiconductor clusters, we do for the present ones not observe a correlation between stability and band gap. Finally, for none of the systems we found a charge separation upon electronic excitation.

Acknowledgments

This work was supported by the German Research Council through project Sp439/11.

-
- ¹ M. Bruchez, M. Moronne, P. Gin, S. Weiss, A. P. Alivisatos, *Science* **281**, 2013 (1998)
 - ² W. C. W. Chan and S. Nie, *Science* **281**, 2016 (1998)
 - ³ G. P. Mitchell, C. A. Mirkin, R. L. Letsinger, *J. Am. Chem. Soc.* **121**, 8122 (1999)
 - ⁴ V. L. Colvin, M. C. Schlamp, and A. P. Alivisatos, *Nature* **374**, 354 (1994)
 - ⁵ B. O. Dabbpussi, M. G. Bawendi, O. Onitsuka, and M. F. Rubner, *Appl. Phys. Lett.* **66**, 1316 (1995)
 - ⁶ M. C. Schlamp, X. G. Peng, A. P. Alivisatos, *J. Appl. Phys.* **82**, 5837 (1997)
 - ⁷ H. Mattoussi, L. H. Radzilowski, B. O. Dabbousi, E. L. Thomas, M. G. Bawendi, M. F. Rubner, *J. Appl. Phys.* **83**, 7965 (1998)
 - ⁸ Lincoln J. Lauhon, Mark S. Gudiksen, Deli Wang and Charles M. Lieber, *Nature* **420**, 57 (2002)
 - ⁹ A. Malachias, S. Kycia, G. Medeiros-Ribeiro, R. Magalhães-Paniago, T. I. Kamins, and R. Stanley Williams, *Phys. Rev. Lett.* **91**, 176101 (2003)
 - ¹⁰ A. Kolobov, H. Oyanagi, N. Usami, S. Tokumitsu, T. Hattori, S. Yamasaki, K. Tanaka. S. Othake, and Y. Shiraki, *Appl. Phys. Lett.* **80**, 488 (2002)
 - ¹¹ M. A. Malik, P. O'Brien, and N. Revaprasadu, *Chem. Mater.* **14**, 2004 (2002)

- ¹² N. A. Hill, S. Pokrant and A. J. Hill, *J. Phys. Chem.* **103**, 3156 (1999)
- ¹³ J. Pérez-Conde and A. K. Bhattacharjee, *Phys. Rev. B* **67**, 235303 (2003)
- ¹⁴ R. N. Musin and Xiao-Qian Wang, *Phys. Rev. B* **71**, 155318 (2005)
- ¹⁵ P. Blaudeck, Th. Frauenheim, D. Porezag, G. Seifert, and E. Fromm, *J. Phys.: Condens. Matter* **4**, 6389 (1992)
- ¹⁶ D. Porezag, Th. Frauenheim, Th. Köhler, G. Seifert, and R. Kaschner, *Phys. Rev. B* **51**, 12947 (1995)
- ¹⁷ G. Seifert, D. Porezag, and Th. Frauenheim. *Int. J. Quant. Chem.* **58**, 185 (1996)
- ¹⁸ G. Pacchioni and J. Koutecky, *J. Chem. Phys.* **84**, 3301 (1986)
- ¹⁹ A. García, C. Elsässer, J. Zhu, S. G. Louie, and M. L. Cohen, *Phys. Rev. B* **46**, 9829 (1992).
- ²⁰ K. Raghavachari, *J. Chem. Phys.* **84**, 5672 (1986)
- ²¹ M. R. Mckay, J. Shumway, and J. Drucker, *J. Appl. Phys.* **99**, 094305 (2006)
- ²² J.-O. Joswig, S. Roy, P. Sarkar, and M. Springborg, *Chem. Phys. Lett.* **365**, 75 (2002)
- ²³ B. Marsen, M. Lonfat, P. Scheier, and K. Sattler, *Phys. Rev. B* **62**, 6892 (2000)
- ²⁴ B. Marsen, M. Lonfat, P. Scheier, and K. Sattler, *J. Electron Spec. and Related Phenomena* **109**, 157 (2000)
- ²⁵ J. Xiang, W. Lu, Y. Hu, Y. Wu, H. Yan, and C. M. Lieber, *Nature* **441**, 489 (2006)
- ²⁶ P. Sarkar, M. Springborg, and G. Seifert, *Chem. Phys. Lett.* **405**, 103 (2005)
- ²⁷ D. V. Melnikov and J. R. Chelikowsky, *Phys. Rev. B* **69**, 113305 (2004)

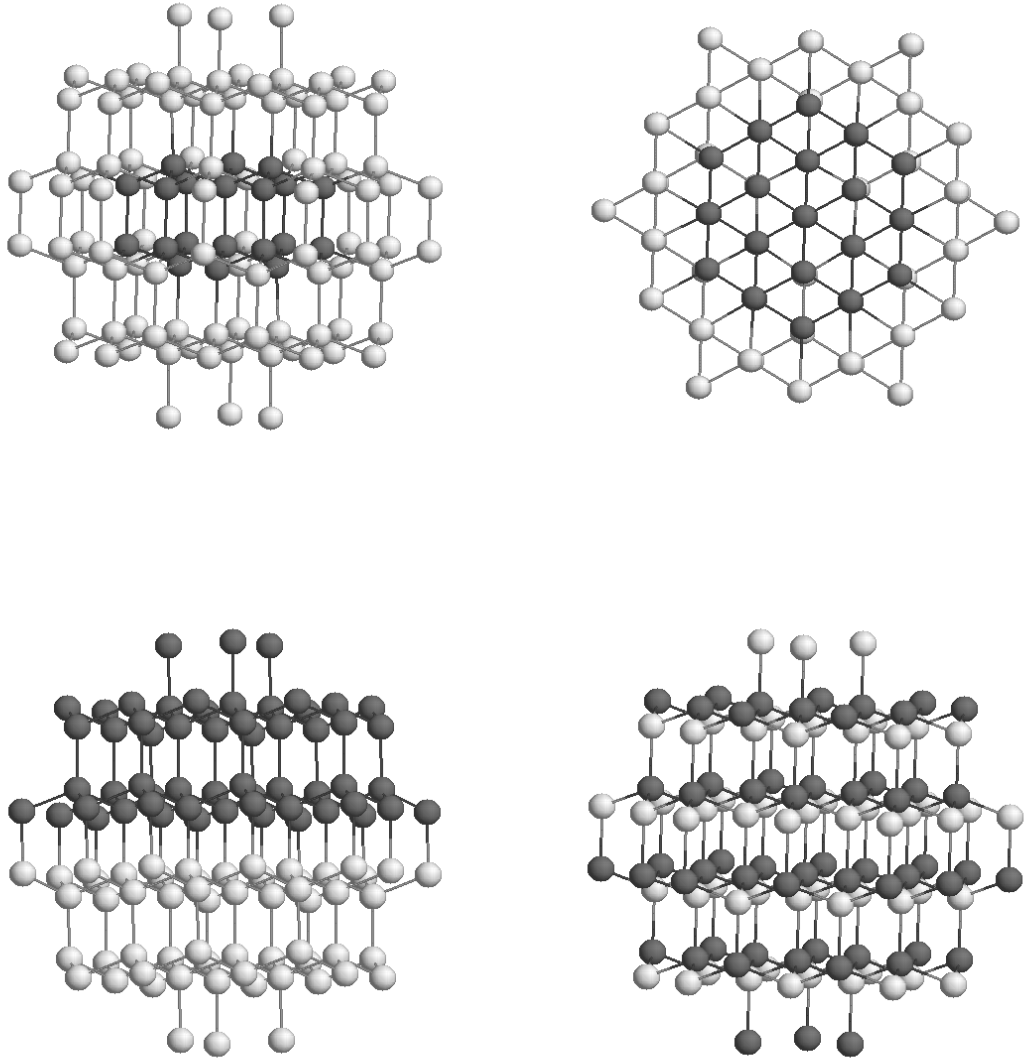


FIG. 1: Ball and stick representation of a representative core/shell structure (upper panel). More and less dark parts represent the core and the shell, respectively. Both the sideview (left panel) and the cross-sectional view (right panel) are presented. Si|Ge (left panel) and homogeneous SiGe (right panel) systems are represented in the lower panel.

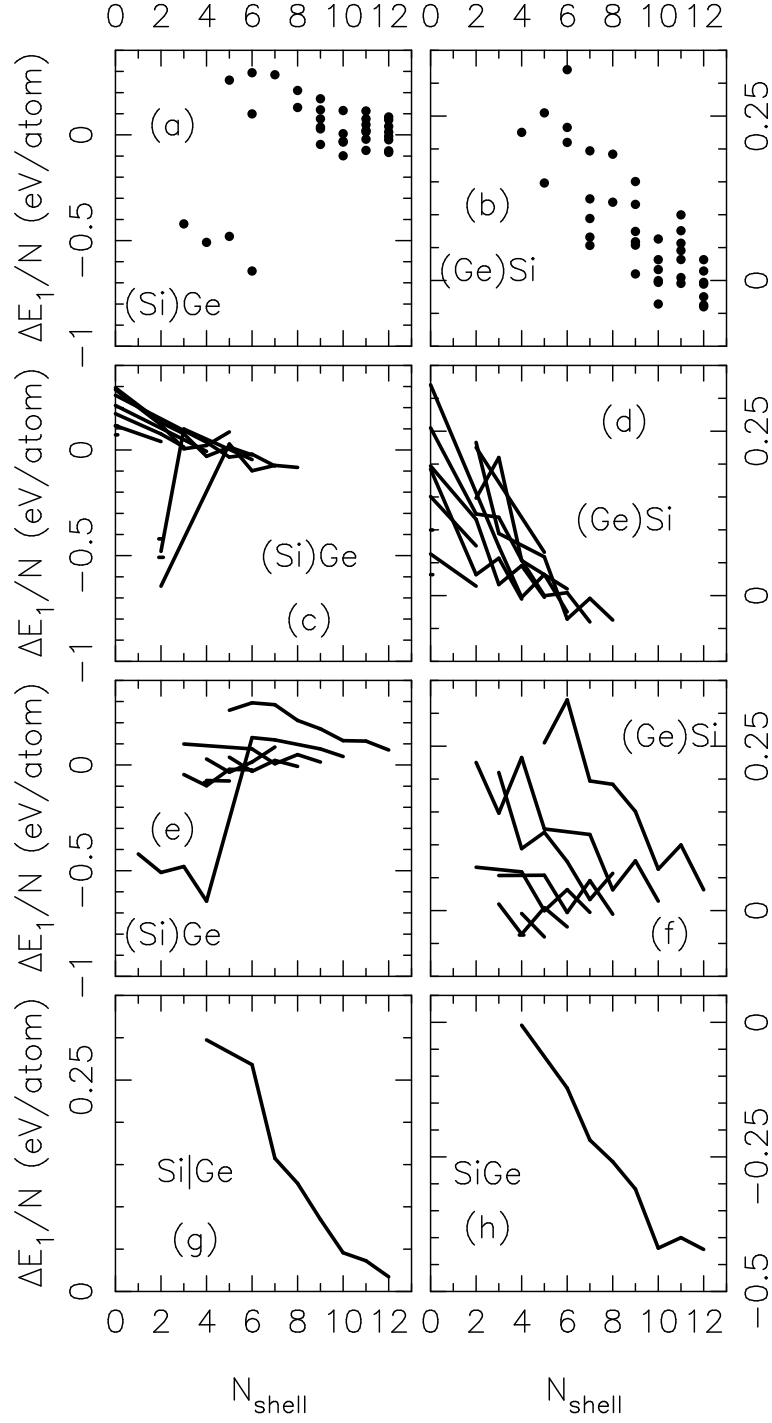


FIG. 2: The variation in the stability energy per atom $\Delta E_1/N$ as a function of the number of atomic shells for the different systems, as indicated in the panel. N_{shell} is the total number of shells, N_t , in (a), (b), (g), and (h), the number of shells in the core, N_c , in (e) and (f), and the number of shells in the shell N_s , in (c) and (d). Finally, the lines in (c)–(f) connect the values for the systems with the same number of atomic shells in (c,d) the core or in (e,f) the shell.

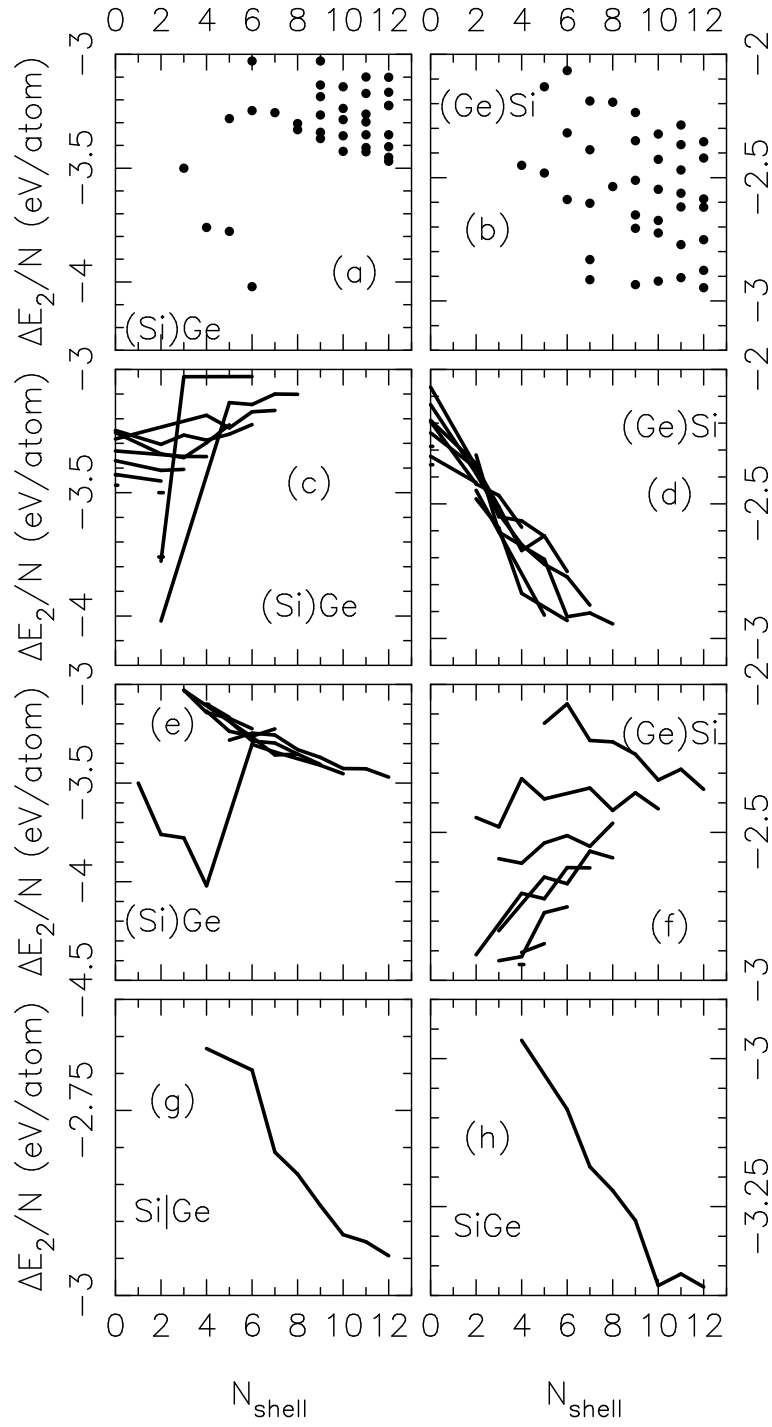


FIG. 3: As Fig. 2, but for the stability energy per atom $\Delta E_2/N$.

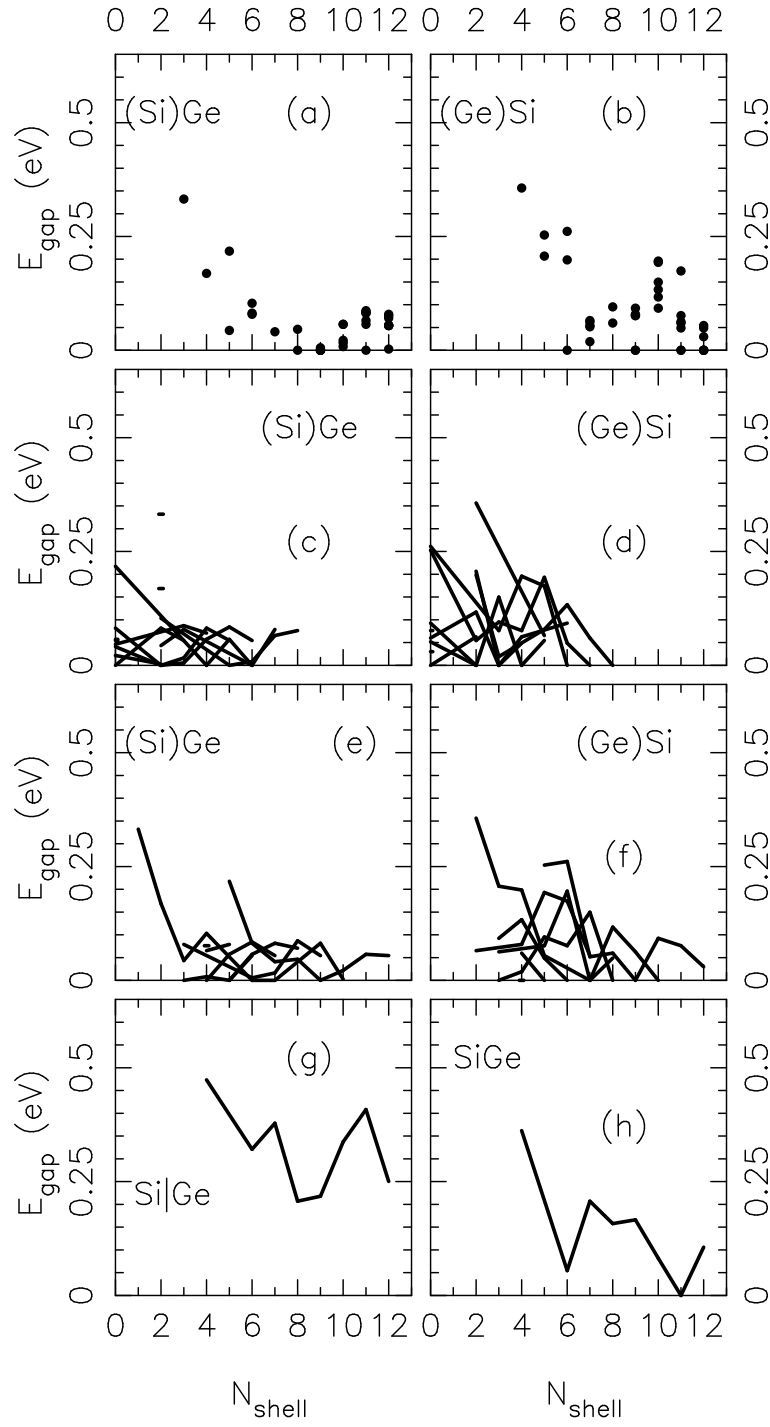


FIG. 4: As Fig. 2, but for the HOMO-LUMO energy gap, E_{gap} .

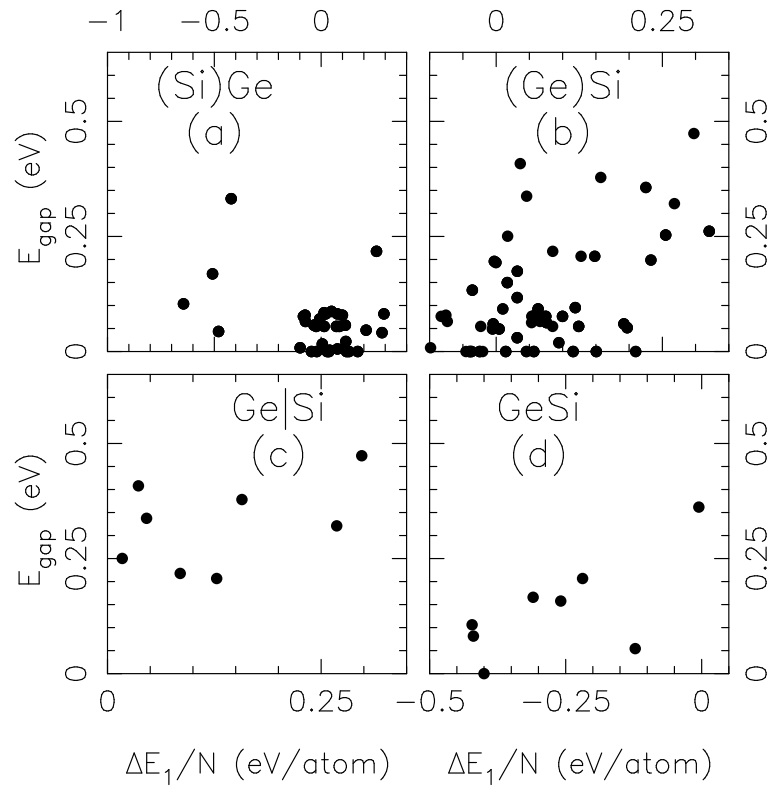


FIG. 5: The HOMO-LUMO energy gap as a function of the stability energy per atom $\Delta E_1/N$ for (a,b) the core/shell systems with (a) Ge covering Si and (b) Si covering Ge as well as for (d) the homogeneous GeSi systems and (c) the Ge|Si systems.

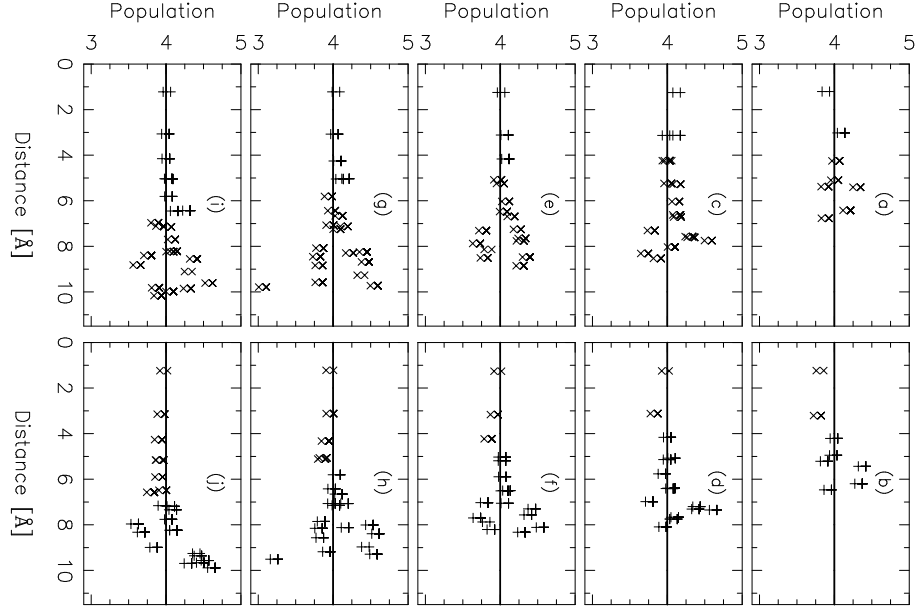


FIG. 6: Radial distribution of Mulliken gross populations of valence electrons of Si (+) and Ge (\times) for (left part) (Si)Ge and (right part) (Ge)Si core/shell particles with n_c atoms in the core and n_s atoms in the shell. (n_c, n_s) equals (a),(b) (8,48), (c),(d) (8,108), (e),(f) (20,110), (g),(h) (32,134), and (i),(j) (56,134). The horizontal solid line marks the value (4) for neutral Si and Ge atoms.

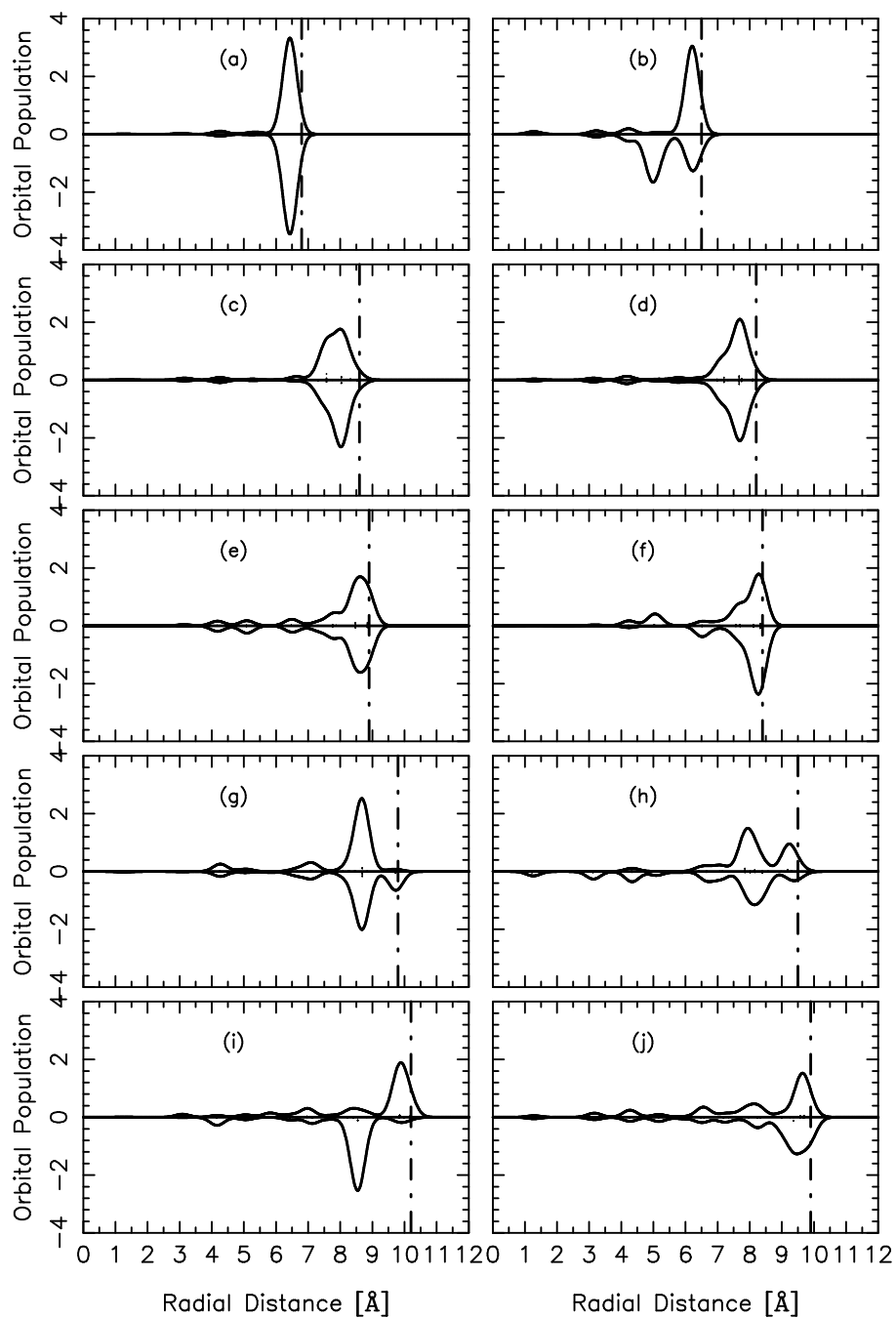


FIG. 7: Schematic presentation of the radial electron distribution of the HOMO (curves pointing upward) and the LUMO (curves pointing downward) for the same systems as in Fig. 6.

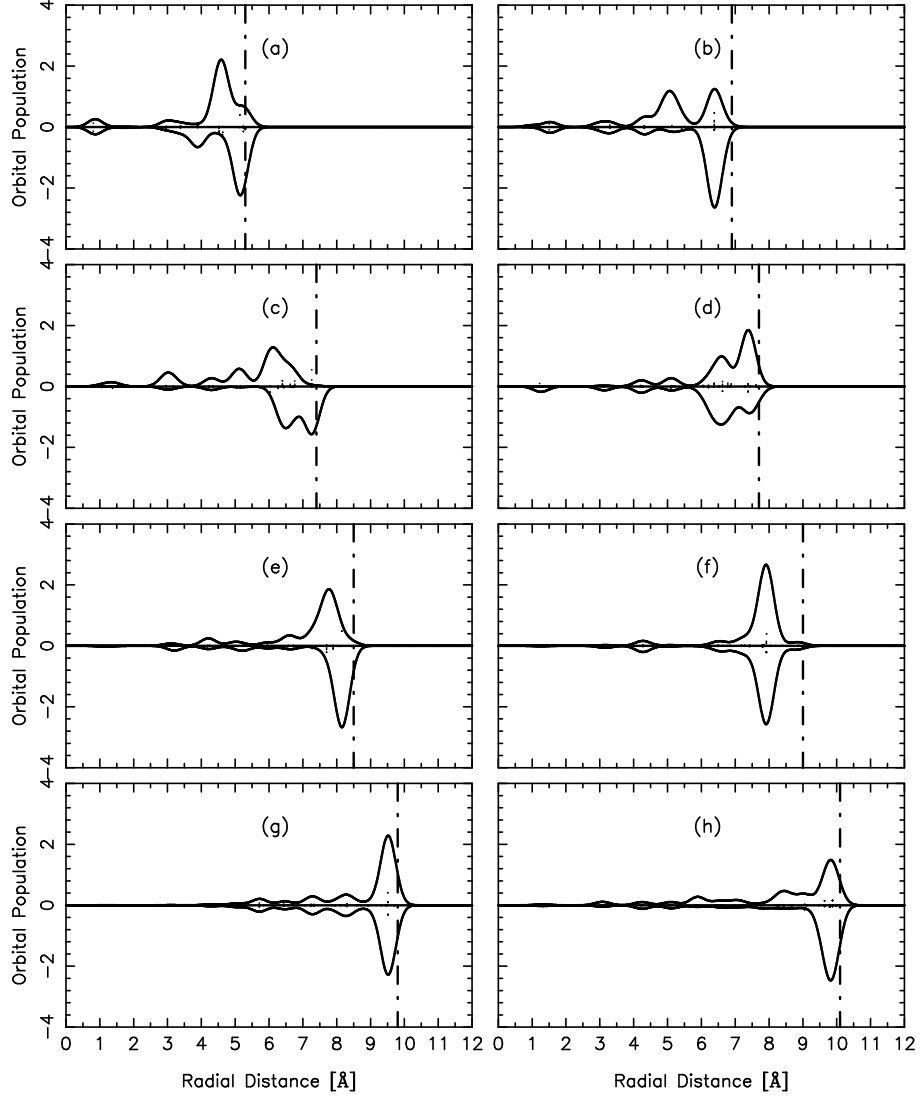


FIG. 8: Schematic presentation of the radial electron distribution of the HOMO (curves pointing upward) and the LUMO (curves pointing downward) for homogeneous SiGe nanoparticles with (a) 32, (b) 56, (c) 74, (d) 86, (e) 116, (f) 130, (g) 166, and (h) 190 atoms.

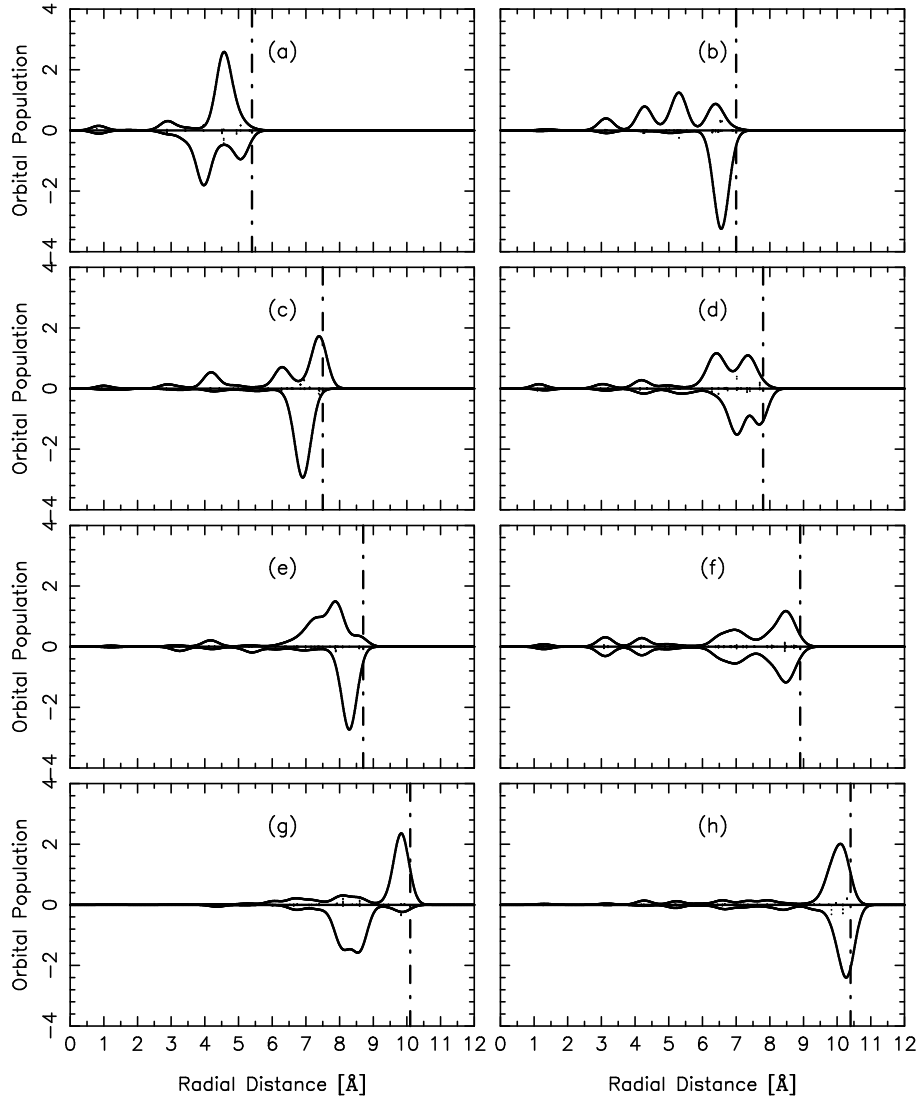


FIG. 9: Schematic presentation of the radial electron distribution of the HOMO (curves pointing upward) and the LUMO (curves pointing downward) for the same number of atoms as Fig. 8 but for Si|Ge nanoparticles.